
INTERNAL WASSERSTEIN DISTANCE FOR ADVERSARIAL ATTACK AND DEFENSE

Mingkui Tan

South China University of Technology
mingkuitan@scut.edu.cn

Shuhai Zhang

South China University of Technology
mszhangshuhai@mail.scut.edu.cn

Jiezhong Cao

South China University of Technology
caojiezhong@gmail.com

Jincheng Li

South China University of Technology
is.lijincheng@gmail.com

Yanwu Xu

Baidu
xmwu@scut.edu.cn

ABSTRACT

Deep neural networks (DNNs) are known to be vulnerable to adversarial attacks that would trigger misclassification of DNNs but may be imperceptible to human perception. Adversarial defense has been an important way to improve the robustness of DNNs. Existing attack methods often construct adversarial examples relying on some metrics like the ℓ_p distance to perturb samples. However, these metrics can be insufficient to conduct adversarial attacks due to their limited perturbations. In this paper, we propose a new internal Wasserstein distance (IWD) to capture the semantic similarity of two samples, and thus it helps to obtain larger perturbations than currently used metrics such as the ℓ_p distance. We then apply the internal Wasserstein distance to perform adversarial attack and defense. In particular, we develop a novel attack method relying on IWD to calculate the similarities between an image and its adversarial examples. In this way, we can generate diverse and semantically similar adversarial examples that are more difficult to defend by existing defense methods. Moreover, we devise a new defense method relying on IWD to learn robust models against unseen adversarial examples. We provide both thorough theoretical and empirical evidence to support our methods.

1 Introduction

Deep neural networks (DNNs) are vulnerable to adversarial examples [1, 2, 3, 4] mainly due to their overfitting nature [5]. Particularly, this issue becomes more severe if we have only limited training data for a specific task. In fact, the neural network tends to fit the training data well and may make an incorrect prediction for an example contaminated by only slight perturbations or transformations. Moreover, the security of deep learning systems is vulnerable to crafted adversarial examples, which may be imperceptible to the human perception but can lead the model to misclassify the output [6, 7]. In practice, adversarial examples can be generated by perturbing or transforming some image pixel values to ensure they maintain the semantic similarity with the original images. Such similarity is a perceptual metric that is often defined by a simple metric such as the ℓ_p distance [8]. However, this ℓ_p metric suffers from two limitations.

First, most attack methods [8, 9, 3] use the ℓ_p distance as a similarity metric to fool a classifier. However, the ℓ_p metric, despite its computational convenience, is ineffective to elaborate all possible adversarial perturbations (e.g., translation, dilation or deformation) due to its insufficient perturbations. Specifically, the attackers always use this metric to ensure that adversarial examples are bounded in a small norm box to keep the semantic consistency of adversarial examples and original ones, which limits the effectiveness of the adversarial perturbations. As shown in Figure 1, adversarial examples crafted with ℓ_∞ using FGSM [8] are often close to the original sample, which may result in an ineffective attack when the sample is distant from the decision boundary. Thus, it is difficult for each image to find an effective adversarial example that causes misclassification of the classifier. Therefore, how to measure the similarity of a sample and its adversarial example is very necessary and important.

Second, models trained merely on ℓ_p adversarial examples are vulnerable to the adversarial examples crafted on the manifold with generative models [10, 11]. One possible reason is that those attack methods, used for generating ℓ_p

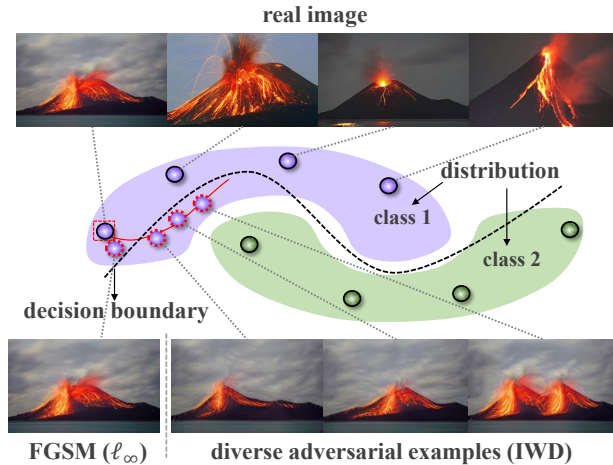


Figure 1: Adversarial examples generated with ℓ_∞ and IWD using FGSM and our method. The ℓ_∞ adversarial examples are close to the original examples, may result in an unsuccessful attack when the sample is far from the decision boundary. In contrast, the IWD adversarial examples are far away from the original ones while keeping the semantic similarity of the samples.

adversarial examples, understand an input image from a one-sided view in Euclidean space and thus may be insufficient to perturb samples on the manifold. In this sense, perturbing a sample on the manifold would be important to achieve a robust model. In this way, we would obtain more diverse and valuable adversarial examples for training. More importantly, diverse adversarial examples can help in covering the blind area of the data distribution to develop robust models [12, 13]. Unfortunately, how to generate diverse adversarial examples and build robust models with them is unknown.

In this paper, we investigate two key questions: 1) how to effectively attack a model on the manifold; and 2) how to build robust models relying on those attacks. Nevertheless, we find the commonly used ℓ_p distance is insufficient when conducting attack and defense to DNNs on the manifold. To address this, we propose an internal Wasserstein distance (IWD). Relying on IWD, we develop a new attack method (called IWDA) to perturb samples on the manifold. Correspondingly, we develop a defense method (called IWDD) to defend against unseen adversarial examples.

The contributions of this paper are summarized as follows:

- We analyze the reasons why the ℓ_p distance is insufficient when doing attacks and defenses. We thus propose an internal Wasserstein distance (IWD) to exploit the internal distribution of data for both attack and defense tasks.
- We propose a novel attack method to craft adversarial examples using the proposed IWD metric. Additionally, we develop a new defense method to improve the robustness of the classifier. Experimental results demonstrate the effectiveness of the proposed methods.
- We analyze the generalization ability of the proposed IWDD. Theoretical and empirical evidence justifies that adversarial examples with more diversity are required in adversarial training.

2 Related Work

2.1 Adversarial Attack

Attack with the ℓ_p perturbation. DNNs are vulnerable to adversarial examples with a perceptible perturbation [1]. Most existing methods [8, 12, 14, 15, 3] attempt to craft adversarial examples with the ℓ_p perturbation. However, these adversarial examples cannot result in a large perturbation that can guarantee successful attacks. Besides, the ℓ_p perturbation is not a good metric of image similarity [16].

Attack with the non- ℓ_p perturbation. To mitigate the limitations of the ℓ_p perturbations, several methods [16, 17, 15, 18, 19, 20] try to craft adversarial examples beyond the ℓ_p perturbations. To this end, [16] propose an ADef algorithm to craft adversarial examples by deforming images iteratively. In addition, [21] iteratively project adversarial examples onto the Wasserstein ball. To develop stronger and faster attacks, [20] apply projected gradient descent and Frank-Wolfe to craft adversarial examples. However, these adversarial examples may lack diversity. In this paper, we propose a novel metric, internal Wasserstein distance (IWD), to generate diverse adversarial examples.

2.2 Adversarial Defense

To address the vulnerability of DNNs, many defense methods [8, 22] have been proposed to defend against adversarial examples. For example, [9] present a projected gradient descent (PGD) training method to improve the resistance of the model to a wide range of attacks. Unfortunately, training with PGD is time-consuming and computationally intensive [23]. To address this, free-PGD [23] and fast-AT [24] speed up the training and improve the robustness of the model.

Recently, PGD adversarial training is a popular method to defend against adversarial examples. However, most studies [25, 26, 27, 28, 29, 13] posit that a robustness-accuracy trade-off may be inevitable in defense methods. For example, [30] theoretically analyze the trade-off between standard risk and adversarial risk and derive a Pareto-optimal trade-off over some specific classes of models in the infinite data with fixed features dimension. In addition, [31] introduce a Nuclear-Norm regularizer to enforce the function smoothing in the vicinity of data samples to achieve an efficient and effective adversarial training method. Moreover, [32] propose a hybrid Langevin Monte Carlo technique to improve the performance of adversarial training. However, these methods are limited in improving the robustness of a classifier due to the limitations of the ℓ_p distance. In this paper, we derive an upper bound to enhance the robustness relying on the IWD.

3 Notation and Motivations

Notation. We use calligraphic letters (*e.g.*, \mathcal{X}) to denote spaces, and bold lower case letters (*e.g.*, \mathbf{x}) to denote vectors. Without loss of generality, we first consider a framework of binary classification, which can be well generalized to the multi-class classification. Let \mathcal{D} be the real data distribution, and $\widehat{\mathcal{D}} = \{(\mathbf{x}_i, \mathbf{y}_i)\}_{i=1}^n \in \mathcal{X} \times \mathcal{Y}$ be the training data, where $\mathbf{x} \in \mathcal{X} \subset \mathbb{R}^m$ denotes the data and $\mathbf{y} \in \{-1, +1\}$ denotes the label. Let $h : \mathcal{X} \rightarrow \mathcal{Y}$ be a classifier learned on $\widehat{\mathcal{D}}$ and valued in $\{-1, +1\}$. Let $\text{diam}(\mathcal{A})$ be the diameter of a set \mathcal{A} . Let $\mathbf{1}\{A\}$ be an indicator function, where $\mathbf{1}\{A\}=1$ if A is true and $\mathbf{1}\{A\}=0$ otherwise. Let $\epsilon(d)$ be a sufficiently small constant with respect to some metric d , and $\mathcal{B}_x(\mathbf{x}, \epsilon(d)) = \{\tilde{\mathbf{x}} \in \mathcal{X} | d(\mathbf{x}, \tilde{\mathbf{x}}) \leq \epsilon(d)\}$ be the $\epsilon(d)$ -neighborhood set of \mathbf{x} . Similarly, let $\mathcal{B}_h(h, \epsilon(d)) = \{\mathbf{x} \in \mathcal{X} | \exists \tilde{\mathbf{x}} \in \mathcal{B}_x(\mathbf{x}, \epsilon(d)) \text{ s.t. } h(\mathbf{x}) \neq h(\tilde{\mathbf{x}})\}$ be the $\epsilon(d)$ -neighborhood set of h , as shown in Figure 2.

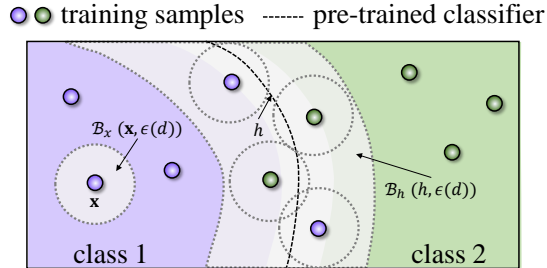


Figure 2: Illustration of notations.

To begin with, we provide the definition of the adversarial example to develop our proposed method.

Definition 1. ($\epsilon(d)$ -adversarial example) Given a sample pair (\mathbf{x}, \mathbf{y}) , the sample \mathbf{x} admits an $\epsilon(d)$ -adversarial example if there exists a sample $\tilde{\mathbf{x}} \in \mathcal{X}$ such that $h(\tilde{\mathbf{x}}) \neq \mathbf{y}$ and $d(\mathbf{x}, \tilde{\mathbf{x}}) \leq \epsilon(d)$, $\epsilon(d) > 0$.

To construct an adversarial example $\tilde{\mathbf{x}}$, most existing methods often use the ℓ_p distance as the metric d . However, this metric is insufficient when conducting attack and defense.

Limitations of the ℓ_p distance for attack and defense. The ℓ_p distance may only ensure that the crafted adversarial examples are close to the original sample due to small perturbations (see Figure 1). When performing the attack, if a sample is far away from the decision boundary, it is difficult to find an effective adversarial example that can fool the classifier. Thus, the ℓ_p distance is insufficient to conduct adversarial attacks when a good classifier can well describe the boundaries of different classes with a large margin.

For defense, most existing methods reinforce the training procedure by searching for adversarial examples relying on the ℓ_p distance. In this way, they try to learn a robust classifier to cover the blind area of the data distribution. However, they may fail to cover the whole data distribution due to the limited range of the ℓ_p perturbation, leading to inferior defense performance. To address these, we propose a new metric in this paper to exploit the internal distribution of data for both attack and defense.

3.1 Internal Wasserstein Distance

As aforementioned, the attack and defense methods relying on the ℓ_p distance are insufficient to perturb the samples. Recently, the Wasserstein distance [33] has been proposed to measure the differences between two given distributions and widely used in generated adversarial networks (GANs) [34].

Definition 2. (1-Wasserstein distance [33]) Given two distributions \mathcal{D} and \mathcal{D}' of \mathbf{x} and \mathbf{x}' , respectively, the Wasserstein distance can be defined as:

$$\widetilde{\mathcal{W}}(\mathcal{D}, \mathcal{D}') = \inf_{\mathbb{T} \in \Pi(\mathcal{D}, \mathcal{D}')} \mathbb{E}_{(\mathbf{x}, \mathbf{x}') \sim \mathbb{T}} [\|\mathbf{x} - \mathbf{x}'\|_1]. \quad (1)$$

Here, Π is a set of all joint distributions \mathbb{T} whose marginal distributions are \mathcal{D} and \mathcal{D}' .

Remark 1. In this paper, we consider 1-Wasserstein distance following [34]. Concretely, the 1-Wasserstein distance has a well-defined dual formulation and can be developed in WGAN [34] using the Kantorovich-Rubinstein duality [33].

Note that while the Wasserstein distance has been widely used in GANs, it is non-trivial to apply it to conduct adversarial attack, since the Wasserstein distance between two samples in Eqn. (1) is difficult to be defined without defining their distributions. To this end, [21] and [20] directly model it as the moving pixel mass from one whole image to another. However, they focus on the changes of global pixels, which may result in a large Wasserstein distance when the internal patch of the image transforms, *e.g.*, swapping the internal patch with each other.

To address this, we propose an internal Wasserstein distance (IWD) to measure the internal distribution distance between a sample \mathbf{x} and its adversarial sample $\tilde{\mathbf{x}}$. Specifically, let $\{\mathbf{u}_i\}_{i=1}^N$ and $\{\mathbf{v}_i\}_{i=1}^N$ be N patches drawn from two samples \mathbf{x} and $\tilde{\mathbf{x}}$, respectively. We define the internal distributions of \mathbf{x} and $\tilde{\mathbf{x}}$ as $\mu = \frac{1}{N} \sum_i \delta_{\mathbf{u}_i}(\mathbf{x})$ and $\nu = \frac{1}{N} \sum_i \delta_{\mathbf{v}_i}(\tilde{\mathbf{x}})$, respectively, where δ is the Dirac distribution [35]. Then, we define the IWD as follows.

Definition 3. (Internal Wasserstein distance) Given internal distributions μ and ν of \mathbf{x} and $\tilde{\mathbf{x}}$, respectively, the internal Wasserstein distance can be defined as:

$$\mathcal{W}(\mathbf{x}, \tilde{\mathbf{x}}) := \inf_{\gamma \in \Gamma(\mu, \nu)} \mathbb{E}_{(\mathbf{u}, \mathbf{v}) \sim \gamma} [\|\mathbf{u} - \mathbf{v}\|_1], \quad (2)$$

where Γ is a set of all joint distributions γ whose marginal distributions are μ and ν .

Remark 2. From the definition, IWD is different from the Wasserstein distance. Specifically, the Wasserstein distance in Eqn. (1) is not able to directly calculate the similarity between two samples \mathbf{x} and $\tilde{\mathbf{x}}$ without defining their distributions. Although [21] and [20] consider this problem as the moving mass from \mathbf{x} to $\tilde{\mathbf{x}}$, this is not necessarily a good measure of image similarity: *e.g.*, swapping the internal patches of $\mathbf{x} = [\mathbf{x}_1, \mathbf{x}_2]$ causes their Wasserstein distance $\mathcal{W}([\mathbf{x}_1, \mathbf{x}_2], [\mathbf{x}_2, \mathbf{x}_1]) > 0$ if $\mathbf{x}_1 \neq \mathbf{x}_2$, which will be zero in our IWD, *i.e.*, $\mathcal{W}([\mathbf{x}_1, \mathbf{x}_2], [\mathbf{x}_2, \mathbf{x}_1]) = 0$.

Definition 3 indicates that IWD captures the semantic similarity of two samples with the help of defining distributions of patches in the image, which thus is able to perturb a sample on the manifold when performing attacks. The following theorem indicates that the IWD can lead to larger transformations than the pixel perturbation (*e.g.*, the ℓ_p distance).

Theorem 1. Let $\epsilon(\ell_p)$ and $\epsilon(\mathcal{W})$ denote the perturbation constants with the ℓ_p distance and IWD, respectively. Then for any $\epsilon(\ell_p) > 0$ ($p > 0$), there exists $\epsilon(\mathcal{W}) \leq \epsilon(\ell_p)$ satisfies:

$$\text{diam}(\mathcal{B}_x(\mathbf{x}, \epsilon(\ell_p))) \leq \text{diam}(\mathcal{B}_x(\mathbf{x}, \epsilon(\mathcal{W}))).$$

Theorem 1 shows that the diameter of the perturbation ball in terms of $\epsilon(\mathcal{W})$ is larger than that in terms of $\epsilon(\ell_p)$. Thus, IWD would have a higher probability to find valid adversarial examples that can cause model misclassification than the ℓ_p distance. In the following, we apply IWD to perform adversarial attack and defense.

4 Adversarial Attack with IWD

In general, the **adversarial attack** aims to learn an adversarial attacker $g(\mathbf{x}, \mathbf{z})$ to confuse a classifier h , where \mathbf{z} can be a random noise vector or other kinds of input. We consider untargeted attack and targeted attack, which can be formulated as the following optimization problems:

$$\underbrace{\max_g \mathcal{L}(h(\tilde{\mathbf{x}})\mathbf{y})}_{\text{untargeted attack}} \quad \text{or} \quad \underbrace{\min_g \mathcal{L}(h(\tilde{\mathbf{x}})\mathbf{y}_t)}_{\text{targeted attack}}, \quad (3)$$

where $\tilde{\mathbf{x}} = g(\mathbf{x}, \mathbf{z}) \in \mathcal{B}_x(\mathbf{x}, \epsilon(d))$, \mathbf{y} is the label of \mathbf{x} and \mathbf{y}_t is the label of the targeted attack, $\mathcal{L}(\cdot)$ is some classification-calibrated loss [36].

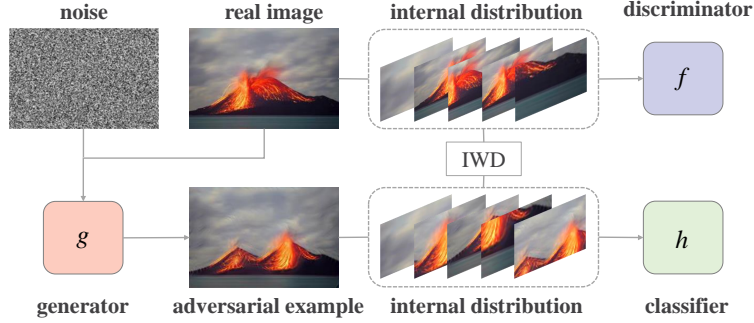


Figure 3: Illustration of our attack method (IWDA). Specifically, g produces an adversarial example such that f cannot distinguish the internal distribution of patches in the generated image from real data, leading to misclassification of the classifier h .

Algorithm 1 Attack method (IWDA).

Input: A sample \mathbf{x} , the hyper-parameters λ and τ , the number of iterations of the discriminator per generator iteration n_{critic} .

Output: The discriminator f , the generator g ,

- 1: **while** not converged **do**
- 2: **for** $t = 0, \dots, n_{\text{critic}}$ **do**
- 3: Adversarial examples $\tilde{\mathbf{x}} = g(\mathbf{x}, \mathbf{z})$, where $\mathbf{z} \sim \mathcal{N}(\mathbf{0}, \mathbf{I})$
- 4: Sample $\hat{\mathbf{x}} \leftarrow \rho \mathbf{x} + (1 - \rho) \tilde{\mathbf{x}}$, where $\rho \sim \mathcal{U}(0, 1)$
- 5: Gradient penalty: $\mathcal{R}_{\text{gp}}(f) = \hat{\mathbb{E}} [(\|\nabla_{\hat{\mathbf{x}}} f(\hat{\mathbf{x}})\|_2 - 1)^2]$
- 6: Update discriminator f by ascending the gradient:

$$\nabla_w \left[\hat{\mathbb{E}}_{\mathbf{u} \sim \mu} [f(\mathbf{u})] - \hat{\mathbb{E}}_{\mathbf{v} \sim \nu} [f(\mathbf{v})] + \lambda \mathcal{R}_{\text{gp}}(f) \right]$$

- 7: **end for**
- 8: Update the generator g by descending the gradient:

$$\nabla_v \left[-\hat{\mathbb{E}}_{\mathbf{v} \sim \nu} f(\mathbf{v}) + \tau \mathcal{L}_c(g; h) \right]$$

- 9: **end while**
-

Relying on IWD, we are able to craft semantically similar but diverse adversarial examples. For example, the crafted adversarial examples of a volcano image (see Figure 1) contain one or more volcanoes with different sizes, shapes and locations. However, it is non-trivial to directly apply IWD to perform adversarial attack to obtain such adversarial examples, since the infimum in Eqn.(2) is highly intractable [34]. To conduct adversarial attack with IWD, we next introduce the objective function for attack.

4.1 Objective Function for Attack

To generate $\epsilon(\mathcal{W})$ -adversarial examples, we propose a new attack method relying on IWD, called IWDA. Figure 1 (a) illustrates the overall scheme of IWDA. Specifically, we optimize an adversarial attack loss $\mathcal{L}_{\text{adv}}(f, g)$ to craft $\epsilon(\mathcal{W})$ -adversarial examples. Meanwhile, we optimize a classification loss $\mathcal{L}_c(g; h)$ such that the classifier misclassifies the adversarial examples. Then, the total objective function can be written as follows:

$$\mathcal{L}(f, g) = \mathcal{L}_{\text{adv}}(f, g) + \tau \mathcal{L}_c(g; h), \quad (4)$$

where τ is a hyper-parameter. Next, we introduce the adversarial attack loss and classification loss.

Adversarial attack loss. In Figure 1 (a), the generator g aims to produce an adversarial example $\tilde{\mathbf{x}} = g(\mathbf{x}, \mathbf{z})$, and then the discriminator f distinguishes the internal distributions of patches in the adversarial example $\tilde{\mathbf{x}}$ and the original image \mathbf{x} . Relying on the internal Wasserstein distance, we propose to optimize the following adversarial loss:

$$\mathcal{L}_{\text{adv}}(f, g) = \max_{\|f\|_L \leq 1} \mathbb{E}_{\mathbf{u} \sim \mu} [f(\mathbf{u})] - \mathbb{E}_{\mathbf{v} \sim \nu} [f(\mathbf{v})], \quad (5)$$

where μ and ν denote the internal distributions of patches in \mathbf{x} and $\tilde{\mathbf{x}}$, respectively. Here, $\|f\|_L$ is the Lipschitz constant of f . In practice, we introduce a gradient penalty [37] to optimize Problem (5) $\mathcal{R}_{\text{gp}}(f) = \hat{\mathbb{E}}[(\|\nabla f(\hat{\mathbf{x}})\| - 1)^2]$ in its dual form.

Algorithm 2 Defense method (IWDD).

Input: Training data $\{\mathbf{x}_i, \mathbf{y}_i\}_{i=1}^n$, the number of epochs T , the batch size m , the hyper-parameters λ, τ, β , the number of iterations of the discriminator per generator iteration n_{critic} .

Output: The classifier h , the discriminator f , the generator g ,

1: **for** $t = 1, \dots, T$ **do**

2: Sample a mini-batch $(\mathbf{x}, \mathbf{y}) \sim \hat{\mathcal{D}}$

3: Generate adversarial examples $\tilde{\mathbf{x}}$ using Alg. 1

4: Construct a set of adversarial examples $\mathcal{B}_x(\epsilon(\mathcal{W}))$

5: Update the discriminator and generator using Alg. 1

$$\nabla_{w,v} \left[-\hat{\mathbb{E}}_{\hat{\mathcal{D}}} [\mathcal{L}(h(\tilde{\mathbf{x}}), \mathbf{y})] \right], \tilde{\mathbf{x}} \in \mathcal{B}_x(\mathbf{x}, \epsilon(\mathcal{W}))$$

6: Update the classifier h by descending the gradient:

$$\nabla_{\theta} \left[\hat{\mathbb{E}}_{\hat{\mathcal{D}}} [\beta \mathcal{L}(h(\mathbf{x}), \mathbf{y}) + \mathcal{L}(h(\tilde{\mathbf{x}}), \mathbf{y})] \right]$$

7: **end for**

Classification loss. The classification loss $\mathcal{L}_c(g; h)$ can be calculated by the distance between the prediction $h(g(\mathbf{x}, \mathbf{z}))$ and the ground truth \mathbf{y} (untargeted attack), or the opposite of the distance between the prediction and the target class \mathbf{y}_t (targeted attack). Then, $\mathcal{L}_c(g; h)$ can be written as:

$$\mathcal{L}_c(g; h) = \begin{cases} -\mathcal{L}(h(g(\mathbf{x}, \mathbf{z}))\mathbf{y}), & \text{untargeted attack,} \\ \mathcal{L}(h(g(\mathbf{x}, \mathbf{z}))\mathbf{y}_t), & \text{targeted attack.} \end{cases} \quad (6)$$

The detailed algorithm is shown in Algorithm 1.

In practice, we select different patches of images by training a pyramid GAN model with different scales progressively in a coarse-to-fine manner. For example, we first set a sliding window (e.g. kernel size = 3) and select N patches of the current image x , where $N = \text{imageLength} \times \text{imageWidth} / \text{kernelSize}^2$. In this sense, the number of patches in different scales is depended on the image size.

Differences with DeepEMD [38]. The idea of comparing patches of images using the Wasserstein distance can be also referred to other works, e.g., DeepEMD. Concretely, DeepEMD calculates the similarity between local features of two images for few-shot learning. In contrast, IWDA measures the Wasserstein distance of the distribution of patches in two images and aims to craft adversarial examples that can confuse the classifier.

5 Adversarial Defense with IWD

Relying on IWD, our proposed method (IWDA) is able to effectively attack the classifier by distribution perturbations on the manifold. Note that the attack and defense are coupled tasks. Essentially, with sufficient adversarial examples, we are able to learn a robust classifier. In this sense, we propose a new defense method with IWD, called IWDD.

5.1 Objective Function for Defense

Mathematically, the **adversarial defense** problem aims to learn a robust classifier h to defend against the attacks from an adversarial generator g to be learned. Following [9, 23], we can learn h and g simultaneously by solving the following minimax problem:

$$\min_h \mathbb{E}_{(\mathbf{x}, \mathbf{y}) \sim \mathcal{D}} \left[\max_g \mathcal{L}(h(\tilde{\mathbf{x}}))\mathbf{y} \right], \text{ s.t. } \tilde{\mathbf{x}} \in \mathcal{B}_x(\mathbf{x}, \epsilon(\ell_p)). \quad (7)$$

However, due to the limitations of the ℓ_p distance, the Solutions like (7) are limited in improving the robustness of a model. By contrast, IWD is able to obtain a large perturbation from Theorem 1. To achieve a robust model, we derive an upper bound to develop our IWDD relying on the IWD.

To begin with, we define the expected classification error as $\mathcal{E}_{\mathcal{D}}(h) = \mathbb{E}_{(\mathbf{x}, \mathbf{y}) \sim \mathcal{D}} [\mathbf{1}\{h(\mathbf{x}) \neq \mathbf{y}\}]$ and let $\mathcal{E}_{\mathcal{D}}^* = \inf_h \mathcal{E}_{\mathcal{D}}(h)$. Following [25], we define the attack classification error as below.

Definition 4. (Attack classification error) Given a sample \mathbf{x} , if there exists an $\epsilon(d)$ -adversarial example $\tilde{\mathbf{x}} \in \mathcal{B}_x(\mathbf{x}, \epsilon(d))$ such that $h(\tilde{\mathbf{x}}) \neq \mathbf{y}$, the attack classification error of a classifier can be defined as:¹

$$\mathcal{E}_{\mathcal{B}_x}(h) = \mathbb{E}_{(\mathbf{x}, \mathbf{y}) \sim \mathcal{D}} [\mathbf{1} \{ \exists \tilde{\mathbf{x}} \in \mathcal{B}_x(\mathbf{x}, \epsilon(d)), \text{ s.t. } h(\tilde{\mathbf{x}}) \neq \mathbf{y} \}].$$

Based on Definition 4, we derive the following upper bound to achieve the robustness of the model.

Theorem 2. (Upper bound) Let $\mathcal{L}(h) = \mathbb{E}[\mathcal{L}(h(\mathbf{x}), \mathbf{y})]$ be the \mathcal{L} -risk of h and its optimum $\mathcal{L}^* = \inf_h \mathcal{L}(h)$. There exists a concave function $\xi(\cdot)$ on $[0, \infty)$ such that $\xi(0) = 0$ and $\xi(\delta) \rightarrow 0$ as $\delta \rightarrow 0^+$, we have the following upper bound:

$$\mathcal{E}_{\mathcal{B}_x}(h) - \mathcal{E}_{\mathcal{D}}^* \leq \xi(\mathcal{L}(h) - \mathcal{L}^*) + \mathbb{E} \left[\sup_{\tilde{\mathbf{x}} \in \mathcal{B}_x(\mathbf{x}, \epsilon(\mathcal{W}))} \mathcal{L}(h(\tilde{\mathbf{x}}), \mathbf{y}) \right].$$

From Theorem 2, we minimize the upper bound such that $\mathcal{E}_{\mathcal{B}_x}(h) - \mathcal{E}_{\mathcal{D}}^*$ can be small. In this way, the attack probability can be guaranteed to be sufficiently small. To this end, we propose a robust minimax objective function as follows:

$$\min_h \mathbb{E}_{(\mathbf{x}, \mathbf{y}) \sim \mathcal{D}} \left[\beta \mathcal{L}(h(\mathbf{x}), \mathbf{y}) + \max_{\tilde{\mathbf{x}} \in \mathcal{B}_x(\mathbf{x}, \epsilon(\mathcal{W}))} \mathcal{L}(h(\tilde{\mathbf{x}}), \mathbf{y}) \right], \quad (8)$$

where $\tilde{\mathbf{x}} = g(\mathbf{x}, \mathbf{z})$, and β is a hyper-parameter in practice. In Problem (8), the first term aims to minimize the natural classification loss between the prediction $h(\mathbf{x})$ and the ground-truth \mathbf{y} , while the second term encourages generating $\epsilon(\mathcal{W})$ -adversarial examples. By optimizing Problem (8), the generated adversarial examples can be covered the data distribution to improve the robustness of the classifier.

Extension to multi-class problems. So far, we only focus on the binary classification problem. Actually, for multi-class problems, a surrogate loss is calibrated if minimizers of the surrogate risk are also minimizers of the 0-1 risk [39]. The multi-class calibrated loss also include the cross-entropy loss [25]. Therefore, we generalize Problem (8) to the multi-class classification problems as:

$$\min_h \mathbb{E}_{(\mathbf{x}, \mathbf{y}) \sim \mathcal{D}} \left[\beta \mathcal{L}(h(\mathbf{x}), \mathbf{y}) + \max_{\tilde{\mathbf{x}} \in \mathcal{B}_x(\mathbf{x}, \epsilon(\mathcal{W}))} \mathcal{L}(h(\tilde{\mathbf{x}}), \mathbf{y}) \right], \quad (9)$$

where $\mathcal{L}(\cdot)$ is the cross-entropy loss. The detailed algorithm is shown in Algorithm 2.

Differences with TRADES [25]. The idea of extending the binary classification to the multi-class classification was also presented in TRADES. However, the perturbation ball they defined in Problem (9) is in the ℓ_p distance and thus they generate adversarial examples by the PGD attack [9]. On the contrary, our IWDD algorithm uses the IWD metric to stimulate diverse adversarial examples to cover the low-density regions of the data, which would lead to better defense performance.

5.2 Minimax Game Analysis

We analyze the generalization performance of our defense method via a minimax game analysis in the setting of Problem (9). To begin with, we give a formal definition of the expected and empirical adversarial risk as follows:

Definition 5. (Adversarial risk) Given a hypothesis $h \in \mathcal{H}$ and the classification boundary neighborhood $\mathcal{B}_h(h, \epsilon(\mathcal{W}))$, the expected adversarial risk can be defined as:

$$\mathcal{R}_{\mathcal{D}}(h) = \mathbb{E}_{(\mathbf{x}, \mathbf{y}) \sim \mathcal{D}} \left[\beta \mathcal{L}(h(\mathbf{x}), \mathbf{y}) + \max_{\tilde{\mathbf{x}} \in \mathcal{B}_x(\mathbf{x}, \epsilon(\mathcal{W}))} \mathcal{L}(h(\tilde{\mathbf{x}}), \mathbf{y}) \right],$$

where \mathcal{D} is the real data distribution. We also define the empirical adversarial risk as $\mathcal{R}_{\hat{\mathcal{D}}}(h)$ over the empirical distribution $\hat{\mathcal{D}}$ with n training data.

Based on this definition, we introduce a transport map [33] to push forward the distribution \mathcal{D} to a new distribution \mathcal{D}' that contains adversarial examples.

Lemma 1. (Equivalence property) Let $\mathcal{D}' = T_{\#} \mathcal{D}$ be a pushforward of the distribution \mathcal{D} by a transport map T . For any hypothesis h , the adversarial risk is equivalent to

$$\mathcal{R}_{\mathcal{D}}(h) = \mathbb{E}_{(\mathbf{x}, \mathbf{y}) \sim \mathcal{D}} [\beta \mathcal{L}(h(\mathbf{x}), \mathbf{y})] + \mathbb{E}_{(\mathbf{x}, \mathbf{y}) \sim \mathcal{D}'} [\mathcal{L}(h(\mathbf{x}), \mathbf{y})].$$

¹We justify the existence of $\epsilon(d)$ -adversarial examples in the supplementary.

Table 1: Comparisons of attack success rate for different attack methods on ImageNet (3-8 lines: untargeted; 9-10 lines: targeted). “-” indicates the method is unsuitable for this type of attack. We report the worst-case accuracy for all the attacks.

Model	Attack success rate (ASR) (%)					
	FGSM	stAdv	EOT	ADef	FWAdv	IWDA
Inception-v3	69.78	99.45	99.73	100.00	98.34	100.00
Inception-v3 (free-PGD)	15.51	69.31	88.12	97.36	76.24	100.00
Inception-v3 (fast-AT)	19.17	73.31	88.72	97.74	84.21	99.34
ResNet-101	89.43	99.73	99.46	100.00	100.00	100.00
ResNet-101 (free-PGD)	18.83	61.42	91.12	97.22	74.58	100.00
ResNet-101 (fast-AT)	17.39	60.54	94.31	97.32	74.25	99.62
Inception-v3 (targeted)	0.27	18.96	48.63	55.77	-	90.66
ResNet-101 (targeted)	1.90	59.35	79.13	87.26	-	94.58

Table 2: Comparisons of attack success rate for different attack methods on tiny ImageNet.

Model	Attack success rate (ASR) (%)			
	FGSM	ADef	FWAdv	IWDA
ResNet-101 (PGD)	9.53	79.77	21.39	91.55
ResNet-101 (TRADES)	7.95	75.43	26.57	92.69

Based on lemma 1, the expected adversarial risk over the distribution \mathcal{D} is equivalent to the standard adversarial risk over the new distribution \mathcal{D}' . For convenience, we let $\tilde{\Psi}=\{\tilde{\psi} : (\mathbf{x}, \mathbf{y})\rightarrow\mathcal{L}(h(\mathbf{x}), \mathbf{y}), (\mathbf{x}, \mathbf{y})\sim\mathcal{D}\}$ and $\Psi=\{\psi : (\mathbf{x}, \mathbf{y})\rightarrow\mathcal{L}(h(\mathbf{x}), \mathbf{y}), (\mathbf{x}, \mathbf{y})\sim\mathcal{D}'\}$, then we derive the following generalization bound.

Theorem 3. (Generalization bound) *Given a bounded instance space $\Omega=\mathcal{X}\times\mathcal{Y}$, i.e., $\text{diam}(\Omega)<\infty$, we assume ψ is upper semi-continuous and uniformly bounded function $0\leq\psi(\mathbf{x})\leq M$, and a constant L exists such that ψ satisfies $\psi(\mathbf{x}') - \psi(\mathbf{x}) \leq L\|\mathbf{x}-\mathbf{x}'\|_2$ for any \mathbf{x}' . For any $\psi \in \Psi$, with $c > 0$ and the probability at least $1 - \delta$, we have*

$$\mathcal{R}_{\mathcal{D}}(h)-\mathcal{R}_{\tilde{\mathcal{D}}}(h)\leq 2\mathfrak{R}\left(\tilde{\Psi}\right)+\frac{24\mathfrak{C}(\Psi)}{\sqrt{n}}+2M\sqrt{\frac{\log(1/\delta)}{2n}}+24c\sqrt{\pi/n}\text{diam}(\Omega),$$

where $\mathfrak{R}(\tilde{\Psi})$ is the Rademacher complexity of $\tilde{\Psi}$, and $\mathfrak{C}(\Psi)$ is the covering number of Ψ [40].

Theorem 3 indicates that the generalization error of our defense model can be bounded by the Rademacher complexity $\mathfrak{R}(\tilde{\Psi})$ and the covering number $\mathfrak{C}(\Psi)$ with a fixed sample size n . When the number of diverse adversarial examples n is sufficiently large, the generalization error bound for our robust model will be small, leading to achieving the robustness to attacks. In this sense, the diversity of adversarial examples is required to cover the whole data distribution to improve defense performance. In contrast, existing defense methods are limited to improving the generalization performance because of lacking diverse adversarial examples.

6 Experiments

Dataset. Following [16], We conduct experiments on ImageNet [41]. In addition, we arbitrarily choose 10 classes from ImageNet (called tiny ImageNet), e.g., barn, megalith, alp, cliff, coral reef, lakeside, seashore, valley, volcano, and coral fungus. Due to the space limitation, the results on CIFAR-10 are provided in the supplementary.

Implementation details. We implement our method based on PyTorch [42] and use the architectures of the models following [43]. Specifically, we use two pre-trained classifiers (i.e., Inception-v3 [44] and ResNet-101 [45]) in the attack methods. During the training, we use an Adam optimizer [46] to update the generator and the discriminator models with $\beta_1=0.5$ and $\beta_2=0.999$ and set the learning rate as 0.0005. For the defense methods, we use an SGD optimizer to train a new classifier with 200 epochs, a learning rate of 0.1, and a batch size of 128. More details of implementation and network architectures are provided in the supplementary.

Baselines and evaluation metrics. We compare our attack method with the non- ℓ_p and ℓ_p attacks. Specifically, the non- ℓ_p attacks include ADef [16], EOT [15], stAdv [19] and FWAdv [20], while the ℓ_p attack includes FGSM [8]. We use attack success rate (ASR) to measure the probability of successfully attacking the pre-trained classifier. For defense methods, we use free-PGD [23], PGD [9], fast-AT [24], TRADES [25] and MART [29] as baseline methods. We calculate the classification accuracy on clean samples and adversarial examples. More details of the settings for these methods are in the supplementary.

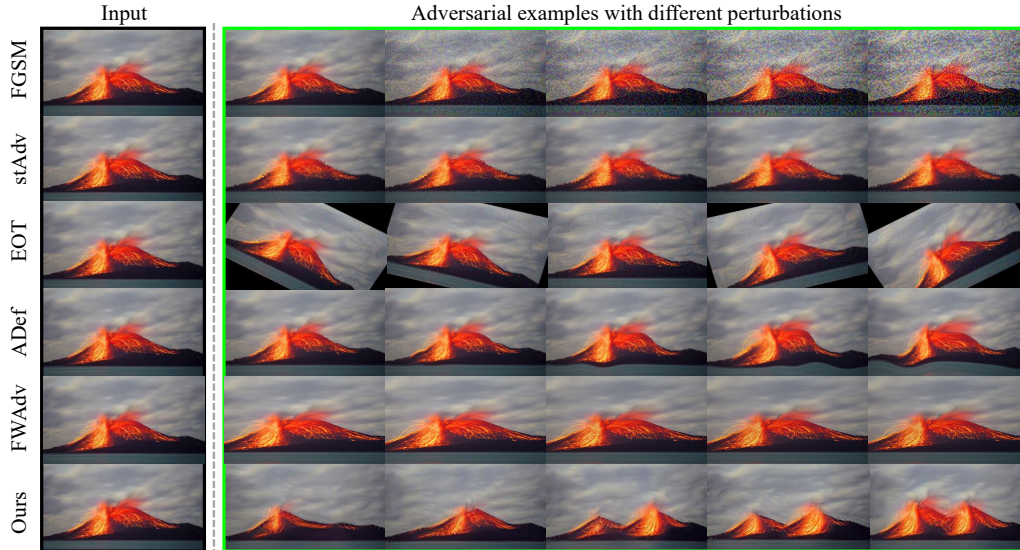


Figure 4: Comparisons of generated untargeted adversarial examples with different intensities of perturbation. (FGSM: step size; stAdv: flow; EOT: rotations; ADef: smoothness; FWAdv: mass shift; Ours: internal Wasserstein distance)

Table 3: Accuracy (%) of robust models on tiny ImageNet. (“natural” training uses only clean data while others use both training data and generated adversarial examples.)

Model	Training method	Clean data	PGD-10	FWAdv
Inception-v3	natural	83.00	0.00	0.00
	free-PGD	62.80	28.40	54.60
	PGD	70.60	45.00	53.20
	IWDD	70.80	46.00	63.40
ResNet-101	natural	79.80	0.00	0.00
	free-PGD	41.40	24.20	36.20
	PGD	69.20	44.00	54.40
	fast-AT	50.80	39.40	44.60
	TRADES	70.00	45.00	51.60
	MART	62.20	44.20	51.20
	IWDD	71.80	45.60	52.00

6.1 Experiments on Adversarial Attack

We consider Inception-v3 and ResNet-101 as classifiers obtained by naturally training. We use free-PGD [23] and fast-AT [24] to train robust models on ImageNet, while PGD [9] and TRADES [25] on tiny ImageNet. Note that we use free-PGD and fast-AT instead of PGD [9] since PGD is inefficient when training on ImageNet [23]. For a fair comparison with different attack methods (ℓ_p and non- ℓ_p), following the settings in [47, 19], we maintain the visual similarity of the adversarial example and the nature one when enforcing attacks.

Quantitative comparison. In Table 1 and Table 2, IWDA achieves the highest ASR than other baselines. It suggests that IWDA is able to generate more effective adversarial examples with the IWD. In contrast, the perturbation based on the ℓ_p by FGSM is insufficient to confuse the classifier. Moreover, EOT, stAdv, ADef and FWAdv based on the non- ℓ_p apply pixel based transformations to improve ASR. However, when attacking a robust model like free-PGD and fast-AT, these methods are difficult to achieve high ASR results since their transformations (*e.g.*, perturbation or distortion) fail to result in a large perturbation in Euclidean space. We provide more attack results in the supplementary.

Qualitative comparison. In Figure 4, our IWDA is able to generate diverse adversarial examples by exploiting the internal distribution of the image. These samples are far away from the input image in Euclidean space and hence cause a large perturbation. Moreover, they are realistic and semantically invariant for human understanding. In this sense, IWDA has good generalization to generate diverse adversarial examples and helps the classifier to understand a real-world image from different views. In contrast, the baselines lack diversity although using a large perturbation to the images. For example, FGSM often destroys the image resolution; EOT keeps the adversarial the same as the original image but changes different rotations; stAdv damages the smoothness of edges of objects; FWAdv reflects

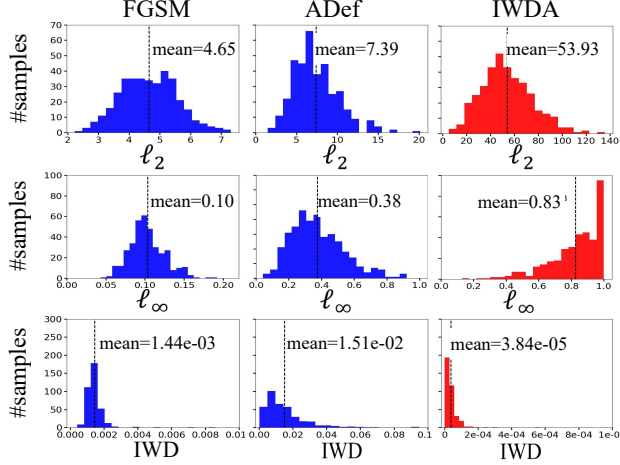


Figure 5: Comparisons of the perturbation for different methods. We use the ℓ_2 distance, the ℓ_∞ distance and IWD to measure the distance between the original samples and perturbed samples.

shapes and contours in original images but also disrupts the image resolution; ADef maintains the smoothness of the image but deforms the original image. Besides, we show the qualitative results of targeted attack in the supplementary.

Comparisons of perturbation. We further compare the perturbation distance of different methods. Under the untargeted attack setting, we use pre-trained ResNet-101 to generate adversarial examples on tiny ImageNet. Specifically, we measure three metrics (*i.e.*, ℓ_2 , ℓ_∞ and IWD) between a sample and its adversarial example. We count the number of perturbed samples over three metrics. In the first two lines of Figure 5, the adversarial examples using the IWDA achieve the highest mean over the ℓ_2 and ℓ_∞ in Euclidean space compared to baseline methods, thus it has larger perturbations to attack the model. More importantly, in the last line, IWDA achieves the smallest IWD values, suggesting that IWDA is powerful in attacking while keeping the high visual similarity of samples.

6.2 Experiments on Adversarial Defense

We use Inception-v3 and ResNet-101 to demonstrate the robustness of IWDD. We train all defense methods on tiny ImageNet and use PGD-10 [9] and FWAdv [20] to attack the models. We present the clean accuracy and the adversarial accuracy.

In Table 3, IWDD achieves a superior or comparable robustness compared to defense baselines. Only against FWAdv on ResNet-101, PGD achieves better performance than IWDD. We believe this is an inherited trade-off between clean accuracy and adversarial accuracy [25, 48]. Other defense baselines like TRADES and MART are limited to improving the generalization performance on both the clean accuracy and adversarial accuracy. From these results, we justify that diverse adversarial examples are required in the adversarial training to improve the robustness of the classifier, which coincides with the result of Theorem 3.

6.3 Ablation Study

We further evaluate the influences of the hyper-parameters τ in Eqn. (4) and β in Eqn. (9) for our methods, respectively. By setting different values of τ and β , we attack the pre-trained ResNet-101 for IWDA and train a robust ResNet-101 for IWDD. The results of attack success rate and validation accuracy are provided in the supplementary. Empirically, when setting $\tau=0.1$, IWDA achieves the highest ASR score and best qualitative results. The performance improves with the increase of τ . Moreover, IWDD obtains the best performance with $\beta=0.1$ when fixing $\tau=0.1$. Thus, We set $\tau=0.1$ and $\beta=0.1$ in practice.

7 Conclusion

In this paper, we have proposed an internal Wasserstein distance (IWD) to measure the similarity between two samples. Relying on IWD, we propose a novel attack method to generate diverse adversarial examples. Meanwhile, we derive an upper bound and propose a new defense method to improve the robustness of the classifier. Moreover, we analyze the generalization performance of our defense method and prove that robustness requires more diverse adversarial examples

in the adversarial training. Extensive experiments on ImageNet confirm the effectiveness of our both attack and defense methods. Furthermore, we expect that a good distance metric will encourage a plethora of researchers to pursue similar tasks in the future.

Acknowledgments

This work was partially supported by Key-Area Research and Development Program of Guangdong Province (2018B010107001, 2019B010155002, 2019B010155001), National Natural Science Foundation of China (NSFC) 61836003 (key project), National Natural Science Foundation of China (NSFC) 62072190, 2017ZT07X183, Tencent AI Lab Rhino-Bird Focused Research Program (No.JR201902), Fundamental Research Funds for the Central Universities D2191240.

References

- [1] Christian Szegedy, Wojciech Zaremba, Ilya Sutskever, Joan Bruna, Dumitru Erhan, Ian Goodfellow, and Rob Fergus. Intriguing properties of neural networks. In *International Conference on Learning Representations*, 2014.
- [2] Ambar Pal and René Vidal. A game theoretic analysis of additive adversarial attacks and defenses. In *Advances in Neural Information Processing Systems*, 2020.
- [3] Francesco Croce and Matthias Hein. Mind the box: 11-apgd for sparse adversarial attacks on image classifiers. In *International Conference on Machine Learning*, 2021.
- [4] Maura Pintor, Fabio Roli, Wieland Brendel, and Battista Biggio. Fast minimum-norm adversarial attacks through adaptive norm constraints. In *Advances in Neural Information Processing Systems*, 2021.
- [5] Leslie Rice, Eric Wong, and J Zico Kolter. Overfitting in adversarially robust deep learning. *arXiv preprint arXiv:2002.11569*, 2020.
- [6] Nicolas Papernot, Patrick McDaniel, Ian Goodfellow, Somesh Jha, Z Berkay Celik, and Ananthram Swami. Practical black-box attacks against machine learning. In *Proceedings of the 2017 ACM on Asia conference on computer and communications security*, pages 506–519, 2017.
- [7] Mahmood Sharif, Sruti Bhagavatula, Lujo Bauer, and Michael K Reiter. Accessorize to a crime: Real and stealthy attacks on state-of-the-art face recognition. In *Proceedings of the 2016 acm sigsac conference on computer and communications security*, pages 1528–1540, 2016.
- [8] Ian J Goodfellow, Jonathon Shlens, and Christian Szegedy. Explaining and harnessing adversarial examples. In *International Conference on Learning Representations*, 2014.
- [9] Aleksander Madry, Aleksandar Makelov, Ludwig Schmidt, Dimitris Tsipras, and Adrian Vladu. Towards deep learning models resistant to adversarial attacks. In *International Conference on Learning Representations*, 2018.
- [10] Yang Song, Rui Shu, Nate Kushman, and Stefano Ermon. Constructing unrestricted adversarial examples with generative models. In *Advances in Neural Information Processing Systems*, 2018.
- [11] Omid Poursaeed, Tianxing Jiang, Harry Yang, Serge J. Belongie, and Ser-Nam Lim. Fine-grained synthesis of unrestricted adversarial examples. *ArXiv*, abs/1911.09058, 2019.
- [12] Francesco Croce and Matthias Hein. Reliable evaluation of adversarial robustness with an ensemble of diverse parameter-free attacks. In *International Conference on Machine Learning*, 2020.
- [13] Divyam Madaan, Jinwoo Shin, and Sung Ju Hwang. Learning to generate noise for multi-attack robustness. In *International Conference on Machine Learning*, 2021.
- [14] F. Croce and M. Hein. Minimally distorted adversarial examples with a fast adaptive boundary attack. In *International Conference on Machine Learning*, 2020.
- [15] Anish Athalye, Logan Engstrom, Andrew Ilyas, and Kevin Kwok. Synthesizing robust adversarial examples. In *International Conference on Machine Learning*, pages 284–293, 2018.
- [16] Rima Alaifari, Giovanni S. Alberti, and Tandri Gauksson. ADef: an iterative algorithm to construct adversarial deformations. In *International Conference on Learning Representations*, 2019.
- [17] Hsueh-Ti Derek Liu, Michael Tao, Chun-Liang Li, Derek Nowrouzezahrai, and Alec Jacobson. Beyond pixel norm-balls: Parametric adversaries using an analytically differentiable renderer. In *International Conference on Learning Representations*, 2019.

- [18] Zhengli Zhao, Dheeru Dua, and Sameer Singh. Generating natural adversarial examples. In *International Conference on Learning Representations*, 2018.
- [19] Chaowei Xiao, Jun-Yan Zhu, Bo Li, Warren He, Mingyan Liu, and Dawn Song. Spatially transformed adversarial examples. In *International Conference on Learning Representations*, 2018.
- [20] Kaiwen Wu, Allen Houze Wang, and Yaoliang Yu. Stronger and faster wasserstein adversarial attacks. In *International Conference on Machine Learning*, pages 10377–10387, 2020.
- [21] Eric Wong, Frank Schmidt, and Zico Kolter. Wasserstein adversarial examples via projected sinkhorn iterations. In *International Conference on Machine Learning*, pages 6808–6817. PMLR, 2019.
- [22] Harini Kannan, Alexey Kurakin, and Ian Goodfellow. Adversarial logit pairing. *arXiv preprint arXiv:1803.06373*, 2018.
- [23] Ali Shafahi, Mahyar Najibi, Amin Ghiasi, Zheng Xu, John Dickerson, Christoph Studer, Larry S Davis, Gavin Taylor, and Tom Goldstein. Adversarial training for free! In *Advances in Neural Information Processing Systems*, 2019.
- [24] Eric Wong, Leslie Rice, and J. Zico Kolter. Fast is better than free: Revisiting adversarial training. In *International Conference on Learning Representations*, 2020.
- [25] Hongyang Zhang, Yaodong Yu, Jiantao Jiao, Eric P Xing, Laurent El Ghaoui, and Michael I Jordan. Theoretically principled trade-off between robustness and accuracy. In *International Conference on Machine Learning*, 2019.
- [26] Aditi Raghunathan, Sang Michael Xie, Fanny Yang, John C. Duchi, and Percy Liang. Understanding and mitigating the tradeoff between robustness and accuracy. In *International Conference on Machine Learning*, 2020.
- [27] Yao-Yuan Yang, Cyrus Rashtchian, Hongyang Zhang, Ruslan Salakhutdinov, and Kamalika Chaudhuri. A Closer Look at Accuracy vs. Robustness. In *Advances in Neural Information Processing Systems*, 2020.
- [28] Jingfeng Zhang, Xilie Xu, Bo Han, Gang Niu, Lizhen Cui, Masashi Sugiyama, and Mohan Kankanhalli. Attacks which do not kill training make adversarial learning stronger. In *International Conference on Machine Learning*, 2020.
- [29] Yisen Wang, Difan Zou, Jinfeng Yi, James Bailey, Xingjun Ma, and Quanquan Gu. Improving adversarial robustness requires revisiting misclassified examples. In *International Conference on Learning Representations*, 2020.
- [30] Mohammad Mehrabi, Adel Javanmard, Ryan A. Rossi, Anup B. Rao, and Tung Mai. Fundamental tradeoffs in distributionally adversarial training. In *International Conference on Machine Learning*, 2021.
- [31] Gaurang Sriramanan, Sravanti Addepalli, Arya Baburaj, and R. Venkatesh Babu. Towards efficient and effective adversarial training. In *Advances in Neural Information Processing Systems*, 2021.
- [32] Alexander Robey, Luiz F. O. Chamon, George J. Pappas, Hamed Hassani, and Alejandro Ribeiro. Adversarial robustness with semi-infinite constrained learning. In *Advances in Neural Information Processing Systems*, 2021.
- [33] Cédric Villani. *Optimal transport: old and new*, volume 338. Springer Science & Business Media, 2008.
- [34] Martin Arjovsky, Soumith Chintala, and Léon Bottou. Wasserstein generative adversarial networks. In *International Conference on Machine Learning*, pages 214–223, 2017.
- [35] HW Alt. Lineare funktionalanalysis. eine anwendungsorientierte einföhrung.. aufl. *Springer-Verlag*, 10:978–3, 2006.
- [36] Peter L Bartlett, Michael I Jordan, and Jon D McAuliffe. Convexity, classification, and risk bounds. *Journal of the American Statistical Association*, 101(473):138–156, 2006.
- [37] Ishaan Gulrajani, Faruk Ahmed, Martin Arjovsky, Vincent Dumoulin, and Aaron C Courville. Improved training of wasserstein gans. In *Advances in Neural Information Processing Systems*, pages 5767–5777, 2017.
- [38] Chi Zhang, Yujun Cai, Guosheng Lin, and Chunhua Shen. Deepemd: Few-shot image classification with differentiable earth mover’s distance and structured classifiers. In *IEEE/CVF Conference on Computer Vision and Pattern Recognition (CVPR)*, June 2020.
- [39] Bernardo Ávila Pires and Csaba Szepesvári. Multiclass classification calibration functions. *arXiv preprint arXiv:1609.06385*, 2016.
- [40] Aman Sinha, Hongseok Namkoong, and John Duchi. Certifiable distributional robustness with principled adversarial training. In *International Conference on Learning Representations*, 2018.
- [41] Olga Russakovsky, Jia Deng, Hao Su, Jonathan Krause, Sanjeev Satheesh, Sean Ma, Zhiheng Huang, Andrej Karpathy, Aditya Khosla, Michael Bernstein, Alexander C. Berg, and Li Fei-Fei. ImageNet Large Scale Visual Recognition Challenge. *International Journal of Computer Vision*, 115(3):211–252, 2015.

- [42] Adam Paszke, Sam Gross, Francisco Massa, Adam Lerer, James Bradbury, Gregory Chanan, Trevor Killeen, Zeming Lin, Natalia Gimelshein, Luca Antiga, Alban Desmaison, Andreas Köpf, Edward Yang, Zachary DeVito, Martin Raison, Alykhan Tejani, Sasank Chilamkurthy, Benoit Steiner, Lu Fang, Junjie Bai, and Soumith Chintala. Pytorch: An imperative style, high-performance deep learning library. In *Advances in Neural Information Processing Systems*, pages 8024–8035, 2019.
- [43] Tamar Rott Shaham, Tali Dekel, and Tomer Michaeli. Singan: Learning a generative model from a single natural image. In *The IEEE International Conference on Computer Vision*, 2019.
- [44] Christian Szegedy, Vincent Vanhoucke, Sergey Ioffe, Jon Shlens, and Zbigniew Wojna. Rethinking the inception architecture for computer vision. In *The IEEE Conference on Computer Vision and Pattern Recognition*, pages 2818–2826, 2016.
- [45] Kaiming He, Xiangyu Zhang, Shaoqing Ren, and Jian Sun. Deep residual learning for image recognition. In *The IEEE Conference on Computer Vision and Pattern Recognition*, 2016.
- [46] Diederik P Kingma and Jimmy Ba. Adam: A method for stochastic optimization. In *International Conference on Learning Representations*, 2015.
- [47] Logan Engstrom, Brandon Tran, Dimitris Tsipras, Ludwig Schmidt, and Aleksander Madry. Exploring the landscape of spatial robustness. In *International Conference on Machine Learning*, 2019.
- [48] Dimitris Tsipras, Shibani Santurkar, Logan Engstrom, Alexander Turner, and Aleksander Madry. Robustness may be at odds with accuracy. In *International Conference on Learning Representations*, 2019.